SACI: Statistical Static Timing Analysis of Coupled Interconnects

Hanif Fatemi, Soroush Abbaspour, Massoud Pedram, Amir H.Ajami*, Emre Tuncer*
Electrical Engineering Department, University of Southern California, Los Angeles, CA
*Magma Design Automation, Santa Clara, CA

Abstract

Process technology and environment-induced variability of gates and wires in VLSI circuits make timing analyses of such circuits a challenging task. Process variation can have a significant impact on both device (front-end of the line) and interconnect (back-end of the line) performance. Statistical static timing analysis techniques are being developed to tackle this important problem. Existing timing analysis tools divide the analysis into interconnect (wire) timing analysis and gate timing analysis. In this paper, we focus on statistical static timing analysis of coupled interconnects where crosstalk noise analysis is unavoidable. We propose a new framework for handling the effect of Gaussian and Non-Gaussian process variations on coupled interconnects. The technique allows for closed-form computation of interconnect delay probability density functions (PDFs) given variations in relevant process parameters such as the line width, metal thickness, and dielectric thickness in the presence of crosstalk noise. To achieve this goal, we express the electrical parameters of the coupled interconnects in a first order (linear) form as function of changes in physical parameters and subsequently use these forms to perform accurate timing and noise analysis to produce the propagation delay and slew in the first-order forms. This work can be easily extended to consider the effect of higher order terms of the sources of variation. Experimental results show that the proposed method is capable of accurately predicting delay variation in a coupled interconnect line.

Categories and Subject Descriptors

B.8.2 [**Performance and Reliability**]: Performance Analysis and Design Aids.

General Terms

Algorithms, Measurement, Performance, Design, Sensitivity.

Keywords

Statistical timing analysis, Crosstalk noise, Coupled interconnect.

1. Introduction

As technology scales down, timing verification of digital integrated circuits becomes an exceedingly challenging task. This is mainly due to the effect of process variation in gate and wire delays. Advanced analysis tools must be developed that are capable of verifying the changes in the circuit timing that stem from various sources of variations. However, static timing analysis (STA) is corner-based. As the number of sources of variations increases, it is impossible to analyze all corners, in this manner; some of the corners omitted by the STA may result in failures after the chip is manufactured [6]. Furthermore, the identification of the corner-point is a complicated task, which is dependent on the precise interconnect and gate structure [6]. Statistical timing analysis (denoted by σTA) provides an effective solution to this key problem [1][3][4][3][6][11].

As technology scales down, interconnects are going to be the limiting factor for high speed digital circuits. They are also responsible for large capacitances, therefore causing major dynamic power dissipation. Finally interconnects are often associated with several signal integrity problems as they can be both the source and the spreading medium for on-chip electrical noise [2] [7].

The drastic down scaling of layout geometries to 90nm and below along with the increase in the operational frequency of VLSI circuits to multiple of GHz have resulted in the aggravation of capacitive crosstalk effects in these circuits. As a result, crosstalk analysis and management have been classified among the most important problems in the IC design flow.

Statistical interconnect timing analysis has been addressed recently. The authors in [2] express the resistance and capacitance of an interconnect line as a linear function of random variables and then use these r.v.'s to compute the circuit moments. These variation-aware moments are used in standard closed-form delay metrics such as the Elmore metric to compute interconnect delay *PDF'*s. In [4], the authors combine known closed-form delay metrics such as Elmore and AWE-based algorithms to take advantage of the efficiency of the first category and the accuracy of the second. Unfortunately, these methods may lead to erroneous results due to the inaccuracy of the closed-form delay metrics. In [3], authors directly calculate the impulse response transfer functions in the variational form and then approximate the timing quantities for a step input as a linear function of the sources of variation. However, the above-mentioned works did not directly address *crosstalk noise* and delay variation in coupled interconnects. Authors of [8] address the problem of analyzing behavior of coupled interconnects with uncertain signal arrival times. The method utilizes delay-change characteristics due to changes in relative arrival time between an aggressor and the victim. The stochastic nature of this work is based on the uncertainty in the arrival time of the inputs and does not address the problem of delay variation as a function of changes in the physical parameters. In [7], authors used simple *L-shaped lumped RC* models for each interconnect line along with a single coupling capacitance. Next, they apply circuit simulation in a statistical sampling framework to determine the voltage distribution of the victim line. However, they do not provide a closed form expression for the delay distribution as a function of changes in the physical parameters. In addition, the electrical model for the coupled interconnect is over-simplistic and may lead to erroneous results.

Crosstalk noise and delay are highly sensitive to back-end process variation such as ILD thickness, metal width and metal

Permission to make digital or hard copies of all or part of this work for personal or classroom use is granted without fee provided that copies are not made or distributed for profit or commercial advantage and that copies bear this notice and the full citation on the first page. To copy otherwise, or republish, to post on servers or to redistribute to lists, requires prior specific permission and/or a fee.
GLSVLSI'06, April 30–May 2, 2006, Philadelphia, Pennsylvania, USA.
Copyright 2006 ACM 1-59593-347-6/06/0004...$5.00.

thickness. Therefore, in this work we express crosstalk noise and delay directly as a function of changes in the physical parameters. The advantages of such a formulation are that it preserves all correlations and that it can be very useful in evaluating noise and delay sensitivities due to changes in various physical dimensions. It can be further utilized for optimization purposes.

The specific contributions of this work are as follows: (i) we propose a method to find a closed form for crosstalk delay distribution as a function of changes in line width, metal thickness and the distance between metal layer and the ground plate (This may include both inter-layer dielectric and inter-metal dielectric thickness). The obtained delay sensitivity coefficients to the sources of variation can be further utilized for optimization purposes. (ii) delay analysis is handled not only for the Gaussian sources of variation but also for the cases where the sources of variation exhibit non-Gaussian distributions. (iii) we use Π model for coupled interconnect which is more accurate in comparison with *L* model used in [8]. (iv) not only the worst case scenario in measuring coupling noise (when the aggressor noise peak matches the victim switching time in the same or opposite direction) but also any arbitrary relative arrival time between the aggressor and the victim can be handled.

Although, the analysis and mathematical formulation in this paper are presented for the case of two coupled lines and Π model is adopted for coupled interconnects, the framework is independent of the model and can be applied to many other coupled structures and electrical models. We also point out that, although in the remainder of this paper we will mainly focus on the first order random variables to represent the performance quantities of interest as a function of process variation, the work itself is not limited to the first-order approximation of these quantities. In fact, it is straightforward to extend the approach to more complex (e.g., second-order) forms for parameter variations.

The remainder of this paper is organized as follows. In section 2, we review the background of statistical timing analysis. We also present the technique which converts a statistical function into a first order form. Delay model for coupled interconnect is presented in section 3. Statistical timing analysis of coupled interconnects is presented in section 4. Experimental results are given in section 5. Conclusions and future work are discussed in section 6. Notice that notations in Table 1 are used throughout this paper.

Table 1: Notation and descriptions

Notation	Description
$hr(t)$	Impulse response in time domain
$HR(s)$	Impulse response in Laplace domain
$sr(t)$	Step response in time domain
$SR(s)$	Step response in Laplace domain
$rr(t)$	Ramp response in time domain
$RR(s)$	Ramp response in Laplace domain
$\overset{\wp}{A}$	Random variable *A* as a function random sources of variations in the general (non- first order) form
$\overset{\triangleleft\triangleright}{A}$	Random variable *A* in the first order form

2. Background

In σTA, it is required to evaluate the distribution of the delay and slew of the critical paths. Conventionally, this goal has been achieved by calculating the mean and variance of the distributions of the delay and slew. However, the sources of variation may exhibit non-Gaussian distributions [11][12] and therefore, result in Non-Gaussian delay distributions. Hence, in addition to calculating the mean and variance of the timing parameters, as a better approximation, we shall also calculate the skewness of their distributions.

***Definition* 1**: The degree of asymmetry of a distribution is called skewness (denoted by κ.) A distribution, or data set, is symmetric if it looks the same to the left and right of the center point. The skewness for a normal distribution is zero. Negative values for the skewness indicate data that are skewed left whereas positive values for the skewness indicate data that are skewed right. By skewed left (right), we mean that the left (right) tail is heavier than the right (left) tail. The *skewness* of a distribution is defined to $\kappa = \mu_3 / \sigma^3$ where μ_3 is the 3rd central moment and σ^2 is the variance (second central moment.).

***Definition* 2:** $X \overset{d_3}{=} Y$ if mean, variance, and the skewness of *X* and *Y* are equal. (i.e., they have the same first three central moments.) Notation $X \sim Dist(\mu, \sigma^2, \kappa)$ is used for approximating the distribution of *X* with its mean, variance and skewness.

The following lemma will be used throughout this paper.

***Lemma* 1:** Suppose $\Delta X_1, \ldots, \Delta X_n$ are *n* independent random variables with distributions $\Delta X_i \sim Dist(\mu=0, \sigma^2=1, \kappa_i)$. Then,

$$\sum_{i=1}^{n} a_i \Delta X_i \overset{d_3}{=} \sqrt{\sum_{i=1}^{n} a_i^2} \, .\Delta X_{eq} \quad \text{where}$$

$$\Delta X_{eq} \sim Dist\left(\mu = 0, \sigma^2 = 1, \kappa = \frac{\sum_{i=1}^{n} a_i^3 \kappa_i}{\left(\sum_{i=1}^{n} a_i^2 \right)^{3/2}} \right)$$

Proof: It is omitted for brevity.

2.1 First order model for electrical and timing parameters

Variation in the physical dimensions of a wire causes change in the resistance and capacitance of the wire, thereby, making the propagation delays and slew times of the wire and its driver to vary accordingly [10]. Therefore, we need to capture the effect of geometric variations on the electrical parameters of the wire. This can be done by a linear approximation as shown below:

$$\overset{\triangleleft\triangleright}{r} = r_0 + a_1 \Delta W + a_2 \Delta T; \quad \overset{\triangleleft\triangleright}{c} = c_0 + c_1 \Delta W + c_2 \Delta T + c_3 \Delta H \qquad (1)$$

where r_0 and c_0 represent nominal resistance and capacitance values, computed when the wire dimensions are at their nominal values. ΔW, ΔT, and ΔH are the variations in metal width, metal thickness and Interlayer Dielectric (ILD) height, respectively. We assume that ΔW, ΔT, and ΔH have known mutually-independent distributions (Note that for the metal layers above *M1, H* includes all of the inter-metal dielectrics plus M1 to substrate ILD). r_i and c_i ($i \neq 0$) are the sensitivity coefficients of resistance and capacitance with respect to the sources of variations, respectively. To compute sensitivity coefficients, we use the empirical equations presented in [13]. These equations have been widely used in industrial extraction tools. With appropriate scaling of the sensitivity coefficients, we can assume that ΔW, ΔT, and ΔH have distributions with μ=0 and σ^2=1 and skewness=κ denoted by $Dist(\mu=0, \sigma^2=1, \kappa)$.

As we discussed earlier, we express the timing quantity of interest as a function of changes in the physical parameters. We explain our method for three sources of variation (metal width, metal thickness and ILD height) but there is no restriction on the number of random variables in the proposed methodology. We present the timing quantity in the following form:

$$\overset{\leftrightarrow}{t} = t_0 + t_W \Delta W + t_T \Delta T + t_H \Delta H \tag{2}$$

where t_0 is the nominal value; ΔW, ΔT and ΔH are the variations in metal width, metal thickness and Interlayer Dielectric (ILD) height respectively. t_W, t_T and t_H are the sensitivity of timing quantity t to each of the sources of variation. By calculating the sensitivity coefficients (t_W, t_T and t_H) and by using Lemma 1 we can compute mean, variance and the skewness of the delay distribution.

Observation: *Invariant Functional Form Property*: This property states that: $y = f(x) \Leftrightarrow \overset{\wp}{Y} = f(\overset{\wp}{X})$. In other words, the form of function f is independent of its input type (deterministic or statistical.)

2.2 Converting a statistical function into the first order form

As mentioned earlier, it is important to represent timing and electrical quantities in the first order form. This in turn enables one to propagate first order sensitivities to different sources of variation through the circuit timing graph [6]. In addition, it makes statistical computation efficient and practical and provides timing diagnostics at a small cost in run time. The remaining question is how to convert a quantity of interest into the first order form. In general, suppose that G is a nonlinear function of m random sources of variation. To represent G in the first order form, we differentiate the function with respect to the sources of variation (ΔX_i's), and we set the variations to zero to find the linear coefficient. Therefore it can be written as:

$$\begin{aligned}
&\overset{\wp}{G}\left(\Delta X_1 ... \Delta X_m\right) \qquad \overset{\wp}{G} \text{ is a non-first order function of sources of variations} \\
&\Rightarrow \overset{\wp}{G} \cong \overset{\wp}{G}\Big|_{\Delta X_l = 0} + \sum_{i=1}^{m} \frac{\partial \overset{\wp}{G}}{\partial \Delta X_i}\Bigg|_{\Delta X_l = 0} \cdot \Delta X_i = \overset{\leftrightarrow}{G} \qquad \text{where } l = 1...m
\end{aligned} \tag{3}$$

where the distribution of $\overset{\leftrightarrow}{G}$ can be calculated using Lemma 1.

As an example, we explain how to calculate *RC* segment propagation delay in the first order form. Let αV_{DD} *crossing time* ($0 \le \alpha \le 1$) denote the instance of time at which a target electrical waveform crosses the αV_{DD} level. Consider an *RC* segment which is driven by a unit step input. Suppose r and c are in the first order form as a function of m sources of variation, ΔX_i's, with the distribution of $\Delta X_i \sim Dist\ (\mu=0, \sigma^2=1, \kappa_i)$. The following equation shows how to derive the first order form, $\overset{\leftrightarrow}{t_\alpha}$, of any αV_{DD} crossing delay for the far-end of an *RC* segment relative to its near end. We can write:

$$\begin{aligned}
&\alpha = 1 - \exp\left(\frac{\overset{\wp}{t_\alpha}}{\overset{\leftrightarrow}{r} \cdot \overset{\leftrightarrow}{c}}\right) \qquad \Rightarrow \overset{\wp}{t_\alpha} = \overset{\leftrightarrow}{r} \cdot \overset{\leftrightarrow}{c} \cdot ln\left(\frac{1}{1-\alpha}\right) \\
&\overset{\leftrightarrow}{t_\alpha} = \overset{\wp}{t_\alpha}\Big|_{\Delta X_i = 0} + \sum_{i=1}^{m} \frac{\partial \overset{\wp}{t_\alpha}}{\partial \Delta X_i}\Bigg|_{\Delta X_i = 0} \cdot \Delta X_i \\
&= \left(r_0 c_0 + \sum_{i=1}^{m} \left(r_i c_0 + r_0 c_i\right) \Delta X_i\right) . ln\left(\frac{1}{1-\alpha}\right)
\end{aligned} \tag{4}$$

By using Lemma 1, we can calculate the distribution of t_α as:

$$t_\alpha \sim Dist\left(\mu_{t_\alpha}; \sigma_{t_\alpha}{}^2; \kappa_{t_\alpha}\right) \qquad \text{where} \qquad \mu_{t_\alpha} = r_0 c_0 \cdot ln\left(\frac{1}{1-\alpha}\right)$$

$$\sigma_{t_\alpha}{}^2 = \sum_{i=1}^{m} \left(r_i^2 c_0^2 + r_0^2 c_i^2\right) \cdot ln^2\left(\frac{1}{1-\alpha}\right) \text{ and } \kappa_{t_\alpha} = \frac{\sum_{i=1}^{m} \left(r_i^3 c_0^3 + r_0^3 c_i^3\right) \cdot \kappa_i}{\left[\sum_{i=1}^{m} \left(r_i^2 c_0^2 + r_0^2 c_i^2\right)\right]^{3/2}}$$

3. Delay Model for Coupled Interconnect

We consider two parallel coupled interconnects with drivers and loads attached as depicted in Figure 1. For our analysis we use an equivalent Π model circuit (as in [9]) for interconnects as shown in Figure 2. We analyze noise and delay at the far end of the interconnects. Although we consider one aggressor line, our analysis can be easily extended to the case of more than one aggressor line for a given victim line.

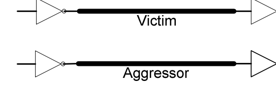

Figure 1. Parallel Coupled interconnects

We use Figure 2 for our analysis purposes. R_{d1} and R_{d2} are the effective on-resistances of drivers of the victim and aggressor lines, respectively; R_1 and R_2 are total resistances of the victim and aggressor lines; C_{v1}, C'_{v2}, C_{a1} and C'_{a2} are the near-end and far-end ground capacitances of the victim and aggressor lines; and finally C_{c1} and C_{c2} are the near-end and far-end coupling capacitances between the two lines. We define: $C_{v2} = C'_{v2} + C_{L1}$ and $C_{a2} = C'_{a2} + C_{L2}$. The voltage at the far end of the victim line in Laplace domain can be written as:

$$\begin{aligned}
V_{vic}(s) &= V_1(s) \cdot H_1(s) + V_2(s) \cdot H_2(s) \\
&= V_1(s) \cdot \frac{1 + a_1 s + a_2 s^2}{1 + b_1 s + b_2 s^2} + V_2(s) \cdot \frac{a_3 s + a_4 s^2}{1 + b_1 s + b_2 s^2}
\end{aligned} \tag{5}$$

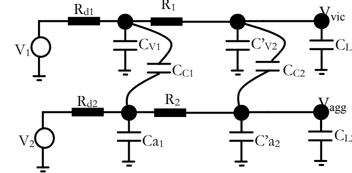

Figure 2. Π Model for coupled interconnects

where a_1, a_2, a_3, a_4, b_1, and b_2 can be represented as functions of the electrical parameters of the circuit [9].

To simplify the presentation of various equations, we set $V_{DD}=1$. We analyze crosstalk noise and delay considering ramp inputs applied to the inputs of aggressor and victim lines. The expression for ramp input in frequency domain is $\frac{1-e^{-sT}}{s^2 T}$ where T is the transition time of the ramp input. Crosstalk noise can be analyzed when the victim line is steady at zero volt, while the aggressor line is switching, for example, from low to high. Therefore, solving Eqn. (5) with $V_1(s)=0$ results in noise computation at the far end of the victim line in frequency domain. The corresponding time domain expression is given by

$$n(t) = L^{-1}\left\{\frac{1 - e^{-sT_{agg}}}{s^2 T_{agg}} \cdot H_2(s)\right\} \tag{6}$$

where L^{-1} indicates the inverse Laplace transform and T_{agg} is the transition time of the aggressor ramp input. Similarly, when the aggressor line is quiet (i.e. $V_2(s)=0$) and the victim line is changing from low to high, the noiseless voltage at the far end of the victim line is given by

$$v_{noiseless}(t) = L^{-1}\left\{\frac{1 - e^{-sT_{vic}}}{s^2 T_{vic}} \cdot H_1(s)\right\} \tag{7}$$

where T_{vic} is the transition time of the aggressor ramp input. When both victim and aggressor lines are switching (in the opposite direction) the voltage at the far end of the victim line is given by

$$v_{vic}(t) = L^{-1}\left\{\frac{1-e^{-sT_{vic}}}{s^2 T_{vic}} \cdot H_1(s)\right\} - L^{-1}\left\{\frac{1-e^{-sT_{agg}}}{s^2 T_{agg}} \cdot e^{-sT_0} \cdot H_2(s)\right\} \qquad (8)$$
$$= v_{noiseless}(t) - n_{T_0}(t)$$

where T_{vic} and T_{agg} are the transition times of the ramp inputs applied to the victim and aggressor lines respectively and T_0 is the relative arrival time of the aggressor with respect to the victim. If the aggressor line is switching in the same direction to the victim line, then Eqn. (8) may be rewritten as $v_{vic}(t) = v_{noiseless}(t) + n_{T_0}(t)$. Note that inverse Laplace transform calculation in Eqns. (6), (7) and (8) are computationally inexpensive and can be easily performed.

4. Statistical Static Timing Analysis of Coupled Interconnect

Problem Statement: Two parallel coupled interconnects with drivers and loads attached are given (cf. Figure 1.) They have been modeled with an equivalent Π circuit as shown in Figure 2. Electrical parameters of the interconnects (*r* and *c*) are in the linear form as a function of changes in physical parameters. Considering ramp inputs applied to the victim and aggressor lines, the objective is to calculate the minimum mean squared error (*MSE*) fit of the distribution of the αV_{DD} (for simplicity of the presentation we assume V_{DD}=1) crossing time at the far end node of the victim line in the first order form as a function of changes in physical parameters such that $E\left\{\left[\overset{\wp}{v}_{vic}(\overset{\lhd\rhd}{t}_\alpha) - \alpha\right]^2\right\}$ is minimized.

$v_{vic}(t)$ is the voltage of the far end node of the victim line in the time domain.

We are interested in calculating the coupled interconnect delay and slew as a function of changes in physical parameters. Assuming ramp inputs are applied to the victim and aggressor lines, the following theorem shows how to evaluate αV_{DD} crossing time at the far end of the victim line in the first order form as a function of changes in physical parameters.

***Theorem*:** Consider coupled interconnects excited by ramp inputs. Assume that the electrical parameter (*r* and *c*) are in the first order form as a function of variation in physical parameters. The minimum *MSE* fit of the distribution of the αV_{DD} crossing time at the far end node of the victim line is calculated as follows:

$$\overset{\lhd\rhd}{t}_\alpha = t_{\alpha,0} + t_{\alpha,W}\Delta W + t_{\alpha,T}\Delta T + t_{\alpha,H}\Delta H \qquad (9)$$

Where,
$$t_{\alpha,0} = v_{vic}^{-1}(\alpha) \qquad (10)$$

$$t_{\alpha,W} = \frac{\Lambda_W(t_{\alpha,0}) - \Psi_W(t_{\alpha,0})}{\frac{1}{T_{vic}}\left(sr_1(t_{\alpha,0}) - sr_1(t_{\alpha,0} - T_{vic})\right) - \frac{1}{T_{agg}}\left(sr_2(t_{\alpha,0} - T_0) - sr_2(t_{\alpha,0} - T_0 - T_{agg})\right)}$$

$$\Lambda_W(t) = L^{-1}\left\{\frac{1-e^{-sT_{vic}}}{s^2 T_{vic}} \cdot \frac{\partial}{\partial \Delta W}\left(\overset{\wp}{H}_1(s)\right)\Bigg|_{\substack{\Delta W=0\\ \Delta T=0\\ \Delta H=0}}\right\} \text{ and} \qquad (11)$$

$$\Psi_W(t) = L^{-1}\left\{\frac{1-e^{-sT_{agg}}}{s^2 T_{agg}} \cdot e^{-sT_0} \cdot \frac{\partial}{\partial \Delta W}\left(\overset{\wp}{H}_2(s)\right)\Bigg|_{\substack{\Delta W=0\\ \Delta T=0\\ \Delta H=0}}\right\}$$

Similarly, by replacing *W* with *T* or *H* (*ΔW* with *ΔT* or *ΔH*), $t_{\alpha,T}$ or $t_{\alpha,H}$ can be computed. Finally, from Lemma 1 the distribution of t_α can be calculated as follows:

$$t_\alpha \sim Dist\left(\begin{array}{c}\mu = t_{\alpha,0}\ ,\ \sigma^2 = t^2_{\alpha,W} + t^2_{\alpha,T} + t^2_{\alpha,H}\ , \\ \kappa = \dfrac{t^3_{\alpha,W}\kappa_W + t^3_{\alpha,T}\kappa_T + t^3_{\alpha,H}\kappa_H}{(t^2_{\alpha,W} + t^2_{\alpha,T} + t^2_{\alpha,H})^{3/2}}\end{array}\right) \qquad (12)$$

Proof: See appendix.

Eqn. (10) (which is simply the inverted form of $v_{vic}(t_{\alpha,0})=\alpha$) implies that to calculate $t_{\alpha,0}$ (i.e., the nominal value of the αV_{DD} crossing time), we must perform delay analysis with all the circuit elements set to their respective nominal values, which has already been solved in STA (cf. section 3.) $H_1(s)$ and $H_2(s)$ are as explained in section 3 where we showed coefficients of $H_1(s)$ and $H_2(s)$ (a_i's and b_j's) as functions of electrical parameters. However, due to the variability of the electrical parameters, a_i's and b_j's are not deterministic scalar values. Instead, by using the invariant functional form property and the technique in section 2.2, we represent them in the first order form. Thus, we can rewrite these transfer functions in Laplace domain as:

$$\overset{\wp}{H}(s) = \sum_{i=0}^{p} \overset{\lhd\rhd}{a}_i s^i \Bigg/ \sum_{j=0}^{q} \overset{\lhd\rhd}{b}_j s^j \qquad (13)$$

$$\text{where } \begin{cases}\overset{\lhd\rhd}{a}_i = a_{i,0} + a_{i,W}\Delta W + a_{i,T}\Delta T + a_{i,H}\Delta H \\ \overset{\lhd\rhd}{b}_j = b_{j,0} + b_{j,W}\Delta W + b_{j,T}\Delta T + b_{j,H}\Delta H\end{cases}$$

where $a_{i,0}$ and $b_{j,0}$ are nominal values of the coefficients of s^i and s^j, respectively; $a_{i,W}$, $a_{i,T}$ and $a_{i,H}$ ($b_{i,W}$, $b_{i,T}$ and $b_{i,H}$) denote sensitivities of a_i (b_i) to ΔW, ΔT, and ΔH, respectively.

$sr_1(t_{\alpha,0})$ and $sr_2(t_{\alpha,0})$ in Eqn. (11) are the step response of $H_1(s)$ and $H_2(s)$ at time $t_{\alpha,0}$ when the circuit is in its nominal condition and they can be calculated as follows:

$$sr_1(t_{\alpha,0}) = L^{-1}\left\{\frac{H_1^{nom}(s)}{s}\right\} \text{ and } sr_2(t_{\alpha,0}) = L^{-1}\left\{\frac{H_2^{nom}(s)}{s}\right\}$$

$\Lambda_W(t_{\alpha,0})$ is equal to the inverse Laplace of the derivative of $H_1(s)$ with respect to ΔW (evaluated when the sources of variations are set to zero) multiplied by the ramp input in frequency domain. After writing $H_1(s)$ in the statistical format as in Eqn. (13), the derivative of $H_1(s)$ with respect to ΔW evaluated at the nominal conditions can be calculated as follows:

$$\frac{\partial}{\partial \Delta W}\left(\overset{\wp}{H}_1(s)\right)\Bigg|_{\substack{\Delta W=0\\ \Delta T=0\\ \Delta H=0}} = \frac{(a_{1,w}s + a_{2,w}s^2)\cdot(1 + b_{1,0}s + b_{2,0}s^2) - (1 + a_{1,0}s + a_{2,0}s^2)\cdot(b_{1,w}s + b_{2,w}s^2)}{(1 + b_{1,0}s + b_{2,0}s^2)^2}$$

Therefore, the evaluation of $\Lambda_W(t_{\alpha,0})$ is not computationally difficult. Similar set of steps can be performed to calculate $\Psi_W(t)$. Finally, Eqn. (12) provides the distribution of t_α. Note that, Eqn. (11) is for the case when the victim and the aggressor lines are switching in the opposite directions. Similarly we can solve the problem for the same type transitions. Figure 3 presents the summary of the algorithm for Statistical static timing Analysis of Coupled Interconnects, called SACI.

```
SACI(Ramp Inputs(T_vic, T_agg, T_0), R_i, C_i)
{
  1.Calculate t_α,0          // Eqn. (10).
  2.Calculate sr_1(t_α,0), sr_2(t_α,0)
  3.For X ∈ {W,T,H}
     3.1. Calculate Λ_X(t_α,0)   // Eqn. (11)
     3.2. Calculate Ψ_X(t_α,0)   // Eqn.(11)
  4.For X ∈ {W,T,H}
        Calculate t_α,X        // Eqn.(11)
  5.Calculate t_α              // Eqn.(9)
  6.Calculate the distribution of t_α   // Eqn.(12)
}
```

Figure 3: General SACI Algorithm

5. Experimental Results

To validate our analysis we have considered two adjacent M4 interconnects used in a real design for 90 nm CMOS technology. We assumed identical interconnects are driven by identical inverters and that the loads at the end of the two lines are also identical inverters. The nominal values of metal width and thickness are 0.2µm and 0.35µm. The nominal value of ILD thickness is 0.45µm and the nominal value of the distance between M4 layer and the ground is 3.0µm. We investigated different configurations for the values of the interconnect length, width, and spacing as reported in Table 2. We assumed 3-sigma variations over their respective nominal values of 25% for the metal width, metal thickness, and the distance between the metal line and the ground plate. We also assumed that the sources of variation are skewed with different skewness values. We assumed fixed pitch size for the adjacent interconnects (i.e. W/2 + spacing + W/2 = constant). We used empirical capacitance modeling equations [13] to compute the capacitances values and the coefficients (sensitivities) of the first order model. The mean, variance, and skewness of the delay at the far end node of the victim line were calculated by using SACI. We used $0.5V_{DD}$ crossing time to compute the interconnect delay from the output of the driver to the next inverter input. In the case of multiple crossings of the $0.5V_{DD}$ level (due to the effect of coupling noise), we considered the last crossing point result. We also performed Hspice-based Monte Carlo simulation with 10,000 samples (for different values of changes in physical parameters) for each test case and recorded the best fit for the mean, variance, and skewness of the delay. The average percentage errors between the results obtained by the Monte Carlo (*Actual*) and the results based on SACI are reported. The nominal values of the interconnect parameters of the model in Figure 2 can be calculated in terms of the interconnect parameters given in Table 2; $R_1=R_2=R_{int}$, $C_{v1}=C_{a1}=C_{gnd}/2$, $C_{v2}=C_{a2}=C_{gnd}/2+C_L$, $C_{c1}=C_{c2}=C_{coupling}/2$. The load capacitance ($C_L$) due to the inverter gate capacitance is 64.5fF for all of the cases. The victim and aggressor driver resistances (R_{d1} and R_{d2}) are assumed to be 200Ω.

Table 2: Interconnect parameters (nominal values) for different cases.

Case	Width (µm)	Spacing (µm)	Length (µm)	R_{int} (Ω)	C_{gnd} (fF)	$C_{coupling}$ (fF)
1	0.2	0.2	800	211.9	26.4	50.19
2	0.2	0.2	4000	1059	131.7	243.7
3	0.4	0.2	8000	1060	415.9	450.3
4	0.2	0.6	800	211.9	57.5	19.7

First, we assume identical transition times for both aggressor and victim lines. The transition time is chosen to be $T_{vic}=T_{agg}=\{40, 72, 104, 136, 168\}$ps. The relative arrival time of the aggressor with respect to the victim line is chosen to be $T_0=\{0.65, 0.70, 0.75, 0.80, .85\}$ns. We assumed the same skewness for all of the three sources of variation and we did our experiment with the skewness of 0, 0.5 and 1. We used SACI to compute the nominal value and the sensitivity of the delay to the sources of variation, and mean, variance and skewness of the delay. Table 3 presents the average percentage errors between the results obtained by the Monte Carlo and the results based on SACI for the case when the aggressor line is switching opposite to the victim line. Table 4 shows the result for the equi-directional transitions on the victim and the aggressor lines. We also considered different transition times for the aggressor and the victim lines. The transition time of the victim line is chosen to be constant (T_{vic}= 104ps) while the aggressor transition times vary from 40ps to 296ps (step size of 32ps.) The relative arrival time of the aggressor with respect to the victim line is also swept from 0.6ns to 0.8ns (step size of 50ps.) The average errors are presented in Table 5 (Table 6) for the opposite (same) transition directions of aggressor and victim lines.

Table 3: Average error (%) for the victim line delay for the opposite transition types with equal transition time

	Delay			
Average error	Case 1	Case 2	Case 3	Case 4
Mean	2.5	4.6	6.8	2.3
Variance	2.7	5.9	7.2	2.7
Skewness	3.3	6.5	7.4	3.1

Table 4: Average error (%) for the victim line delay for the same transition type with equal transition time

	Delay			
Average error	Case 1	Case 2	Case 3	Case 4
Mean	2.4	4.1	6.5	2.1
Variance	2.8	5.3	7.3	2.6
Skewness	3.4	6.1	7.7	2.9

Case 3 shows larger errors due to longer interconnect, and we see smaller error for cases 1 and 4. Case 4 has the smallest coupling capacitance, and therefore, it exhibits smaller crosstalk noise as well. Note that the SACI algorithm is on average 120 times faster than the Monte Carlo-based approach.

Table 5: Average error (%) for the victim line delay for the opposite transition types with different transition time

	Delay			
Average error	Case 1	Case 2	Case 3	Case 4
Mean	2.7	4.5	6.1	2.4
Variance	3.1	5.1	7.1	3.0
Skewness	3.6	6.2	7.7	3.4

Table 6: Average error (%) for the victim line delay for the same transition types with different transition time

	Delay			
Average error	Case 1	Case 2	Case 3	Case 4
Mean	2.8	4.4	6.4	2.5
Variance	3.5	5.0	7.3	2.6
Skewness	3.6	6.5	7.7	2.9

6. Conclusion

We proposed a new framework for handling the effect of Gaussian and Non-Gaussian process variation on coupled interconnects. We expressed the electrical parameters of the coupled interconnects in the first order forms as a function of changes in physical parameters. We utilized these forms to calculate the closed-form formula of the victim line delay distribution as a function of changes in the sources of variation. Experimental results showed that the proposed method is able to accurately predict delay variation through a coupled interconnect while the run time is 120 times faster than the Monte Carlo simulation with 10^4 samples.

7. References

[1] R. Nassif, "Modeling and Analysis of Manufacturing Variations," *CICC*, 2001.

[2] K. Agarwal, D. Sylvester, D. Blaauw, F. Liu, S. Nassif, S. Vrudhula, "Variational delay metrics for interconnect timing analysis," DAC, 2004.

[3] S. Abbaspour, H. Fatemi, M. Pedram, "Parameterized block-based non-Gaussian statistical interconnect timing analysis," DATE, 2006.

[4] S. Abbaspour, H. Fatemi, M. Pedram, "VITA: Variation-aware interconnect timing analysis for symmetric and skewed sources of variation considering variational ramp input," GLSVLSI, 2005.

[5] Agarwal, A.; Dartu, F.; Blaauw, D.;"Statistical gate delay model considering multiple input switching", DAC, 2004.

[6] Visweswariah, C.; Ravindran, K.; Kalafala, K.; Walker, S.G.; Narayan, S.;"First-order incremental block-based statistical timing analysis", DAC, 2004.

[7] M. Martina, G. Masera, "A statistical Model for Estimating the Effect of Process Variation on Crosstalk Noise," SLIP 2004

[8] T. Chern, A. Hajjar, "Statistical Timing Analysis of Coupled Interconnect Using Quadratic Delay-Change Characteristics" TCAD of Integrated Circuits and Systems, 2004.

[9] A. Kahng, S. Muddu, D. Vidhani, "Noise and Delay Uncertainty Studies for Coupled RC Interconnects" ASIC/SOC Conf., 1999.

[10] Y. Liu, S. R. Nassif, L. T. Pileggi, and A. J. Strojwas, "Impact of Interconnect Variations on the Clock Skew of a Gigahertz Microprocessor," DAC, 2000.

[11] X. Li, J. Le, P. Gopalakrishnan, and L. T. Pileggi, "Asymptotic Probability Extraction for Non-Normal Distributions of Circuit Performance," ICCAD, 2004.

[12] H. Chang, V. Zolotov, C. Visweswariah, and S. Narayan, "Parameterized block-based statistical timing analysis with non-Gaussian and nonlinear parameters", DAC, 2005.

[13] J. Chern, J. Huang, L. Arledge, P. Li, and P. Yang, "Multilevel Metal Capacitance Models for CAD Design Synthesis Systems," IEEE Electron Devices Letters, 1992.

8. Appendix

***Definition* 3:** The inverse of the Laplace transform can be calculated as:

$$F(t)=\frac{1}{2\pi i}\int_{\gamma-i\infty}^{\gamma+i\infty} f(s).e^{st}ds \tag{14}$$

where γ is a vertical contour in the complex plane chosen so that all singularities of *f(s)* are to the left of it.

***Proof of Theorem*:** Since $v_{vic}(t_\alpha)$ is a random variable, we must find t_α in the linear form *s.t.*

$$E\left\{\left[\tilde{v}_{vic}\left(\hat{t}_\alpha\right)-\alpha\right]^2\right\}=E\left\{\left[\tilde{v}_{noiseless}(\hat{t}_\alpha)-n_{T_0}(\hat{t}_\alpha)-\alpha\right]^2\right\}\text{is minimized} \tag{15}$$

The above nonlinear stochastic equations are not easy to evaluate, therefore, we approximate $v_{vic}(t_\alpha)$ with:

$$\begin{aligned}
&\tilde{v}_{vic}(\hat{t}_\alpha)\cong\\
&\tilde{v}_{vic}\Big|_{\substack{\Delta W=0\\ \Delta T=0\\ \Delta H=0}}+\frac{\partial\tilde{v}_{vic}}{\partial\Delta W}\Big|_{\substack{\Delta W=0\\ \Delta T=0\\ \Delta H=0}}\cdot\Delta W+\frac{\partial\tilde{v}_{vic}}{\partial\Delta T}\Big|_{\substack{\Delta W=0\\ \Delta T=0\\ \Delta H=0}}\cdot\Delta T+\frac{\partial\tilde{v}_{vic}}{\partial\Delta H}\Big|_{\substack{\Delta W=0\\ \Delta T=0\\ \Delta H=0}}\cdot\Delta H=\\
&\tilde{v}_{noiseless}\Big|_{\substack{\Delta W=0\\ \Delta T=0\\ \Delta H=0}}-\tilde{n}_{T_0}\Big|_{\substack{\Delta W=0\\ \Delta T=0\\ \Delta H=0}}+\left(\frac{\partial\tilde{v}_{noiseless}}{\partial\Delta W}\Big|_{\substack{\Delta W=0\\ \Delta T=0\\ \Delta H=0}}-\frac{\partial\tilde{n}_{T_0}}{\partial\Delta W}\Big|_{\substack{\Delta W=0\\ \Delta T=0\\ \Delta H=0}}\right)\cdot\Delta W+\\
&\left(\frac{\partial\tilde{v}_{noiseless}}{\partial\Delta T}\Big|_{\substack{\Delta W=0\\ \Delta T=0\\ \Delta H=0}}-\frac{\partial\tilde{n}_{T_0}}{\partial\Delta T}\Big|_{\substack{\Delta W=0\\ \Delta T=0\\ \Delta H=0}}\right)\cdot\Delta T+\left(\frac{\partial\tilde{v}_{noiseless}}{\partial\Delta H}\Big|_{\substack{\Delta W=0\\ \Delta T=0\\ \Delta H=0}}-\frac{\partial\tilde{n}_{T_0}}{\partial\Delta H}\Big|_{\substack{\Delta W=0\\ \Delta T=0\\ \Delta H=0}}\right)\cdot\Delta H
\end{aligned} \tag{16}$$

The distribution of our independent random variables (ΔW*,* Δ*T* and Δ*H*) are in the form of $\Delta X_i \sim Dist(\mu=0, \sigma^2=1, \kappa_i)$. Therefore, we have $E(\Delta X_i^2)=1$ and $E(\Delta X_i.\,\Delta X_j)=0$. Hence, to satisfy the minimization in Eqn.(15), we have the following conditions;

$$\tilde{v}_{noiseless}\Big|_{\substack{\Delta W=0\\ \Delta T=0\\ \Delta H=0}}-\tilde{n}_{T_0}\Big|_{\substack{\Delta W=0\\ \Delta T=0\\ \Delta H=0}}=\alpha \text{ and}$$

$$\text{minimize}\left\{\sum_{\Delta X\in\{\Delta W,\Delta T,\Delta H\}}\left(\frac{\partial\tilde{v}_{noiseless}}{\partial\Delta X}\Big|_{\substack{\Delta W=0\\ \Delta T=0\\ \Delta H=0}}-\frac{\partial\tilde{n}_{T_0}}{\partial\Delta X}\Big|_{\substack{\Delta W=0\\ \Delta T=0\\ \Delta H=0}}\right)^2\right\}$$

Therefore,

$$\tilde{v}_{vic}\Big|_{\substack{\Delta W=0\\ \Delta T=0\\ \Delta H=0}}=\tilde{v}_{noiseless}\Big|_{\substack{\Delta W=0\\ \Delta T=0\\ \Delta H=0}}-\tilde{n}_{T_0}\Big|_{\substack{\Delta W=0\\ \Delta T=0\\ \Delta H=0}}=\alpha \tag{17}$$

$$\begin{aligned}
&\frac{\partial\tilde{v}_{noiseless}}{\partial\Delta W}\Big|_{\substack{\Delta W=0\\ \Delta T=0\\ \Delta H=0}}-\frac{\partial\tilde{n}_{T_0}}{\partial\Delta W}\Big|_{\substack{\Delta W=0\\ \Delta T=0\\ \Delta H=0}}=0\ ,\ \frac{\partial\tilde{v}_{noiseless}}{\partial\Delta T}\Big|_{\substack{\Delta W=0\\ \Delta T=0\\ \Delta H=0}}-\frac{\partial\tilde{n}_{T_0}}{\partial\Delta T}\Big|_{\substack{\Delta W=0\\ \Delta T=0\\ \Delta H=0}}=0\\
&\text{and}\quad\frac{\partial\tilde{v}_{noiseless}}{\partial\Delta H}\Big|_{\substack{\Delta W=0\\ \Delta T=0\\ \Delta H=0}}-\frac{\partial\tilde{n}_{T_0}}{\partial\Delta H}\Big|_{\substack{\Delta W=0\\ \Delta T=0\\ \Delta H=0}}=0
\end{aligned} \tag{18}$$

Eqn. (17) means that to calculate $t_{\alpha,0}$ we must perform delay analysis for ramp inputs with all the circuit elements set to their respective nominal values. By using definition 3, the first condition in Eqn. (18) may be treated as follows:

$$\begin{aligned}
&\frac{\partial\tilde{v}_{noiseless}}{\partial\Delta W}\Big|_{\substack{\Delta W=0\\ \Delta T=0\\ \Delta H=0}}-\frac{\partial\tilde{n}_{T_0}}{\partial\Delta W}\Big|_{\substack{\Delta W=0\\ \Delta T=0\\ \Delta H=0}}=0\Rightarrow\frac{\partial}{\partial\Delta W}\left(\frac{1}{2\pi i}\int_{\gamma-i\infty}^{\gamma+i\infty}\frac{1-e^{-sT_{vic}}}{s^2T_{vic}}\cdot\tilde{H}_1(s)\cdot e^{s\hat{t}_\alpha}ds\right)\Big|_{\substack{\Delta W=0\\ \Delta T=0\\ \Delta H=0}}\\
&-\frac{\partial}{\partial\Delta W}\left(\frac{1}{2\pi i}\int_{\gamma-i\infty}^{\gamma+i\infty}\frac{1-e^{-sT_{agg}}}{s^2T_{agg}}\cdot e^{-sT_0}\cdot\tilde{H}_2(s)\cdot e^{s\hat{t}_\alpha}ds\right)\Big|_{\substack{\Delta W=0\\ \Delta T=0\\ \Delta H=0}}=0\Rightarrow\\
&\frac{1}{2\pi i}\int_{\gamma-i\infty}^{\gamma+i\infty}\frac{1-e^{-sT_{vic}}}{s^2T_{vic}}\cdot\frac{\partial}{\partial\Delta W}\left(\tilde{H}_1(s)\right)\Big|_{\substack{\Delta W=0\\ \Delta T=0\\ \Delta H=0}}\cdot e^{st_{\alpha,0}}ds+\\
&t_{\alpha,W}\cdot\frac{1}{2\pi i}\int_{\gamma-i\infty}^{\gamma+i\infty}\frac{1-e^{-sT_{vic}}}{sT_{vic}}\cdot H_1^{nom}(s)\cdot e^{st_{\alpha,0}}ds-\\
&\frac{1}{2\pi i}\int_{\gamma-i\infty}^{\gamma+i\infty}\frac{1-e^{-sT_{agg}}}{s^2T_{agg}}\cdot e^{-T_0s}\cdot\frac{\partial}{\partial\Delta W}\left(\tilde{H}_2(s)\right)\Big|_{\substack{\Delta W=0\\ \Delta T=0\\ \Delta H=0}}\cdot e^{st_{\alpha,0}}ds-\\
&t_{\alpha,W}\cdot\frac{1}{2\pi i}\int_{\gamma-i\infty}^{\gamma+i\infty}\frac{1-e^{-sT_{agg}}}{sT_{agg}}\cdot e^{-T_0s}\cdot H_2^{nom}(s)\cdot e^{st_{\alpha,0}}ds=0
\end{aligned}$$

Therefore,

$$\begin{aligned}
&t_{\alpha,W}=\psi/\phi\ \text{ where }\ \psi=\frac{1}{2\pi i}\int_{\gamma-i\infty}^{\gamma+i\infty}\frac{1-e^{-sT_{vic}}}{s^2T_{vic}}\cdot\frac{\partial}{\partial\Delta W}\left(\tilde{H}_1(s)\right)\Big|_{\substack{\Delta W=0\\ \Delta T=0\\ \Delta H=0}}\cdot e^{st_{\alpha,0}}ds-\\
&\qquad\frac{1}{2\pi i}\int_{\gamma-i\infty}^{\gamma+i\infty}\frac{1-e^{-sT_{agg}}}{s^2T_{agg}}\cdot e^{-T_0s}\cdot\frac{\partial}{\partial\Delta W}\left(\tilde{H}_2(s)\right)\Big|_{\substack{\Delta W=0\\ \Delta T=0\\ \Delta H=0}}\cdot e^{st_{\alpha,0}}ds\\
&\text{and}\quad\phi=\frac{1}{2\pi i}\int_{\gamma-i\infty}^{\gamma+i\infty}\frac{1-e^{-sT_{vic}}}{sT_{vic}}\cdot H_1^{nom}(s)\cdot e^{st_{\alpha,0}}ds-\\
&\qquad\frac{1}{2\pi i}\int_{\gamma-i\infty}^{\gamma+i\infty}\frac{1-e^{-sT_{agg}}}{sT_{agg}}\cdot e^{-T_0s}\cdot H_2^{nom}(s)\cdot e^{st_{\alpha,0}}ds
\end{aligned}$$

which proves Eqn (11). Similarly, the second and the third conditions in Eqn.(18) will result in computing $t_{\alpha,T}$ and $t_{\alpha,H}$. ■